8-Aza-7-deazaguanine nucleosides and oligonucleotides with octadiynyl side chains: synthesis, functionalization by the azide-alkyne 'click' reaction and nucleobase specific fluorescence quenching of coumarin dye conjugates†

Frank Seela,*[a,b] Hai Xiong,[a,b] Peter Leonard[a] and Simone Budow[a]

Received 9th December 2008, Accepted 15th January 2009
First published as an Advance Article on the web 2nd March 2009
DOI: 10.1039/b822041g

Oligonucleotides incorporating 7-(octa-1,7-diynyl) derivatives of 8-aza-7-deaza-2′-deoxyguanosine (**2d**) were prepared by solid-phase synthesis. The side chain of **2d** was introduced by the *Sonogashira* cross coupling reaction and phosphoramidites (**3a**, **3b**) were synthesized. Duplexes containing **2d** are more stabilized compared to those incorporating the non-functionalized 8-aza-7-deaza-2′-deoxyguanosine (**2a**) demonstrating that these side chains have steric freedom in duplex DNA. Nucleoside **2d** as well as **2d**-containing oligonucleotides were conjugated to the non-fluorescent 3-azido-7-hydroxycoumarin **15** by the Huisgen-Meldal-Sharpless 'click' reaction. Pyrazolo[3,4-*d*]pyrimidine nucleoside conjugate **16** shows a much higher fluorescence intensity than that of the corresponding pyrrolo[2,3-*d*]pyrimidine derivative **17**. The quenching in the dye conjugate **17** was found to be stronger on the stage of monomeric conjugates than in single-stranded or duplex DNA. Nucleobase-dye contact complexes are suggested which are more favourable in the monomeric state than in the DNA chain when the nucleobase is part of the stack. The side chains with the bulky dye conjugates are well accommodated in DNA duplexes thereby forming hybrids which are slightly more stable than canonical DNA.

Introduction

The Huisgen-Meldal-Sharpless 'click' reaction has emerged as a convenient and effective approach for the preparation of a diversity of new molecules with various functionalities performed under simple reaction conditions. The reaction is orthogonal to most of the common biomolecule substituents and chemoselective under Cu(I) catalysis.[1] Thus, the protocol is particularly attractive to be applied in drug design,[2] molecular diagnostics[3,4] polymer synthesis, material science,[5–10] and other areas of chemistry and chemical biology.[11–13]

Recently, we reported on the synthesis of oligonucleotides incorporating 7-deaza-7-(octa-1,7-diynyl)-2′-deoxyguanosine (**1**) (purine numbering is used in the results and discussion section). The side chains bearing terminal triple bonds were conjugated with various azides including the dye 3-azido-7-hydroxycoumarin by the Huisgen-Meldal-Sharpless 'click' reaction.[11c,14] Spectroscopic studies showed that the fluorescence is strongly quenched when the DNA nucleobase belongs to the class of pyrrolo[2,3-*d*]pyrimdines. An electron transfer from the nucleobase to the dye moiety was suggested.[14] Thus, it was anticipated that other nucleobases having different redox potentials may not show such drawback. Pyrazolo[3,4-*d*]pyrimidine nucleosides offer properties which make them applicable as alternative systems.[15] They show similar base pairing characteristics and can be functionalized at the 7-position. 8-Aza-7-deazapurine (pyrazolo[3,4-*d*]pyrimidine) nucleosides have already been incorporated into DNA including 7-propynyl and 7-halogeno derivatives.[16–18] It was shown that the 8-aza-7-deaza-2′-deoxyguanosine residues **2a–c** form stable base pairs with dC giving steric freedom to 7-substituents to be well accommodated in the major groove of duplex DNA.[18] Usually, 7-substituted nucleosides form more stable duplexes than the non-functionalized ones.[18–22] Thus, pyrazolo[3,4-*d*]pyrimidine nucleosides can be considered as purine nucleoside shape mimics which will not disturb the DNA duplex structure.

This manuscript reports on the synthesis of 8-aza-7-deaza-7-(octa-1,7-diynyl)-2′-deoxyguanosine (**2d**), its conversion into the phosphoramidite building blocks (**3a**,**b**) and their application in solid-phase oligonucleotide synthesis (Fig. 1). Studies regarding base pairing and fluorescence properties were carried out on oligonucleotides incorporating nucleoside **2d**. The azide-alkyne 'click' reaction for the dye conjugation with 3-azido-7-hydroxycoumarin on nucleosides and oligonucleotides with side chains having terminal triple bonds was studied according to Scheme 1. Fluorescence enhancement of the oligonucleotide coumarin dye conjugates is expected for oligonucleotides containing pyrazolo[3,4-*d*]pyrimidine dye conjugates compared to pyrrolo[2,3-*d*]pyrimidine derivatives.

[a]*Laboratory of Bioorganic Chemistry and Chemical Biology, Center for Nanotechnology, Heisenbergstraße 11, 48149, Münster, Germany. E-mail: Frank.Seela@uni-osnabrueck.de, Seela@uni-muenster.de; Web: www.seela.net; Fax: +49 (0)251-53406-857; Tel: +49 (0)251-53406-500*
[b]*Laboratorium für Organische und Bioorganische Chemie, Institut für Chemie, Universität Osnabrück, Barbarastraße 7, 49069, Osnabrück, Germany*

† Electronic supplementary information (ESI) available: UV spectrum of nucleoside **2d**, pK_a-values of nucleosides, HPLC profile of an artificial mixture of nucleosides and ^{13}C NMR spectra of compounds **2d**, **4a**, **5a**, **4b**, **5b**, **16** and **17**. See DOI: 10.1039/b822041g

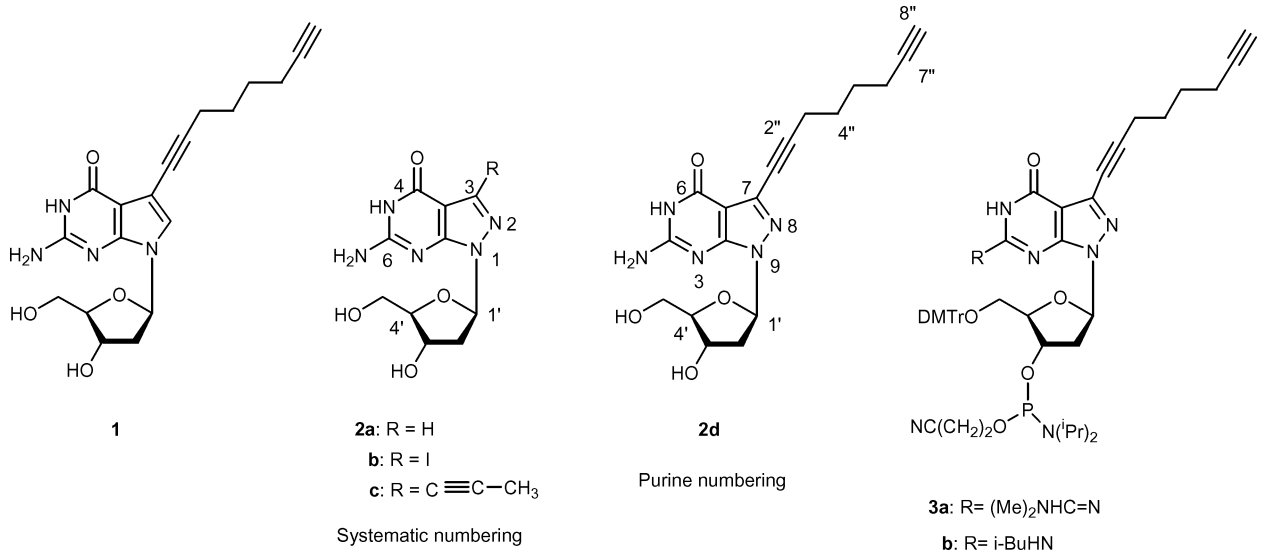

Fig. 1

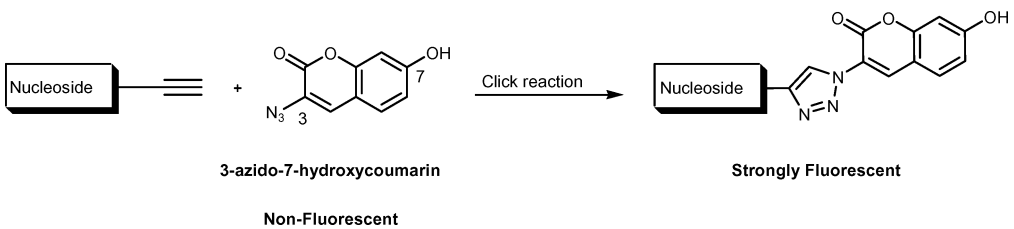

Scheme 1 Copper(I)-catalyzed azide-alkyne cycloaddition.

Results and discussion

1. Synthesis and characterisation of nucleosides

The 7-iodinated 8-aza-7-deaza-2′-deoxyguanosine **2b** served as starting material for the synthesis of the phosphoramidites **3a**,**b**.[15–17] Compound **2b** was employed in the *Sonogashira* cross-coupling reaction resulting in the formation of derivative **2d** (Scheme 2). The reaction was performed in dry DMF in the presence of Et_3N, $[Pd^0(PPh_3)_4]$ and CuI, with a five-fold excess of 1,7-octadiyne.[23,24] Due to the excessive diyne only the terminal C≡C bond was functionalized and compound **2d** was isolated in 52% yield. Next, derivative **2d** was protected at the 2-amino group with either the *N*,*N*-dimethylaminomethylidene or isobutyryl residue affording the protected intermediates **4a** or **4b** in similar yields (88% *vs.* 89%). Both compounds were converted to the 5′-*O*-DMT-derivatives **5a** and **5b** under standard reaction conditions. Phosphitylation yielded the phosphoramidites **3a** and **3b** (63% and 72%, respectively).

All compounds were characterized by either elemental analyses or mass spectra, ^{1}H- and ^{13}C-NMR spectra. The ^{13}C-NMR chemical shifts are listed in Table 1, the ^{1}H-^{13}C-coupling constants were determined from ^{1}H-^{13}C gated decoupled spectra (see Table 6, experimental section). These assignments are in agreement with literature values of propynyl compounds.[18] The intact structure of the octa-1,7-diynyl side chain was confirmed by ^{13}C-NMR spectra showing four signals of the methylene groups (27.1, 27.0, 18.3 and 17.3 ppm) and four signals for the triple bond carbons (**2d**: 71.4, 73.2, 84.4, 100.1 ppm; Table 1), confirmed by inverted signals of distortionless enhancement by polarization transfer (DEPT-135) spectra. From this it was concluded that the triple bonds are not affected by the Pd-assisted *Sonogashira* cross coupling (allene formation).

Pyrazolo[3,4-*d*]pyrimidine nucleosides show significantly altered pK_a values compared to pyrrolo[2,3-*d*]pyrimidine or purine counterparts. Consequently, the pK_a-value of compound **2d** was measured UV-spectrophotometrically and compared with already existing data of 7-deazapurine and 8-aza-7-deazapurine nucleosides (Table S1, see supporting information). The representative titration profile of compound **2d** is shown in Figure S1 (supporting information). From the data of Table S1 it is obvious that lactam protons of the pyrazolo[3,4-*d*]pyrimidine nucleosides are more acidic than those of pyrrolo[2,3-*d*]pyrimidine nucleosides. The 7-substituents have almost no influence on the pK_a-values which is different in case of 5-substituted pyrimidine nucleosides, *e.g.* 2′-deoxyuridine derivatives which are strongly affected by the electronic properties of the side chain.[14]

2. Synthesis, characterization and duplex stability of oligonucleotides

We reported on the influence of substituents of 5-substituted pyrimidines and 7-substituted 7-deazapurines containing halogens or alkynyl groups on the duplex stability.[14,27] It was shown that nucleoside analogues with bromo or iodo substituents and propynyl chains attached to the 7-position of pyrrolo[2,3-*d*]pyrimidines or pyrazolo[3,4-*d*]pyrimidines are well accommodated in the major groove of DNA and increase the thermal stability of duplexes by

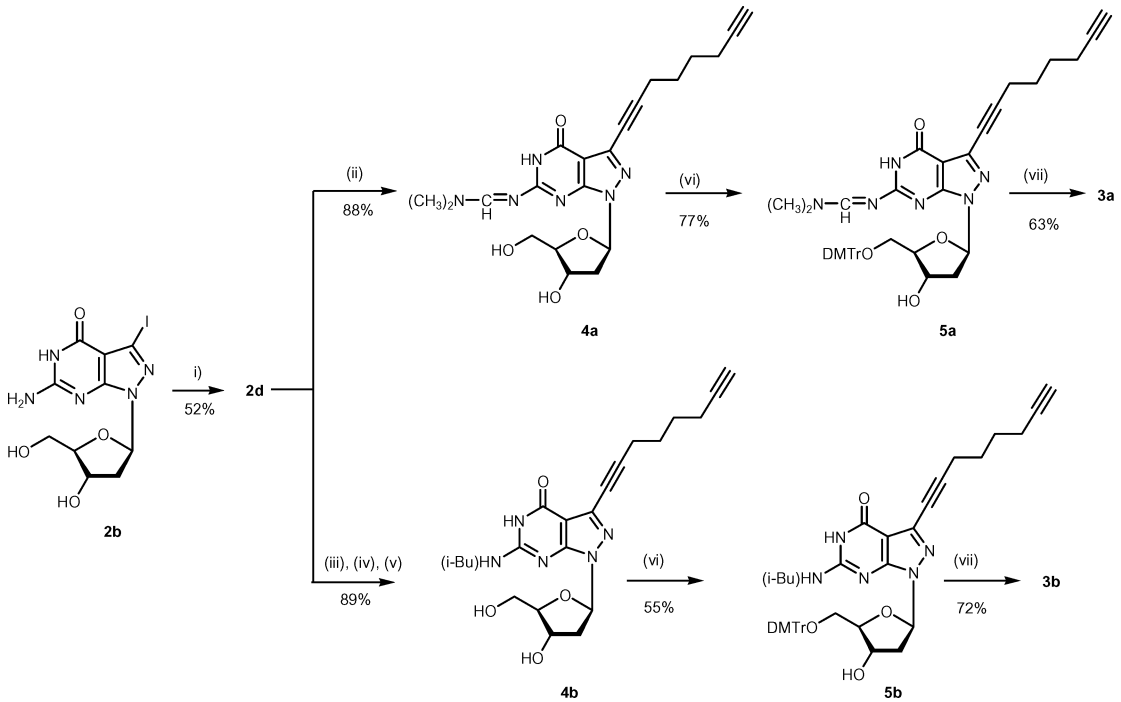

Scheme 2 *Reagents and conditions*: i) octa-1,7-diyne, [$Pd^0[P(Ph_3)_4]$], CuI, DMF, Et_3N, rt, 12 h; (ii) *N*,*N*-dimethylformamide dimethyl acetal, MeOH, rt, 2 h; (iii) HMDS, rt, 3 h; (iv) *i*-Bu_2O, rt, overnight; (v) MeOH, 1 h; (vi) 4,4′-dimethoxytriphenylmethyl chloride, anhydrous pyridine, (*i*-Pr)$_2$EtN, rt; (vii) 2-cyanoethyl-*N*,*N*-diisopropylchlorophosphoramidite, anhydrous CH_2Cl_2, (*i*-Pr)$_2$EtN, rt.

Table 1 ^{13}C-NMR chemical shifts of 8-aza-7-deaza-2′-deoxyguanosine derivatives[a]

	C(2)[b] C(6)[c]	C(4)[b] C(7a)[c]	C(5)[b] C(3a)[c]	C(6)[b] C(4)[c]	C(7)[b] C(3)[c]	C≡C	CH_2	CH_3	C(1′)	C(2′)	C(3′)	C(4′)	C(5′)
2d	155.2	155.5[d]	93.4	157.2[d]	130.5	100.1, 84.4, 73.2, 71.4	27.1, 27.0 18.3, 17.3	—	83.2	38.5	71.0	87.5	62.5
4a	154.6	158.7[d]	93.6	159.5[d]	130.6	102.5, 84.4, 73.7, 71.4	27.2, 27.1, 18.3, 17.4	34.9	83.3	38.5	71.1	87.6	62.5
5a	154.6	158.7[d]	93.1	159.5[d]	130.3	102.5, 85.2, 73.4, 70.6	27.1, 27.0, 18.3, 17.3	34.8	84.3	38.5	71.4	83.0	64.3
4b	150.4	152.8[d]	94.4	155.1[d]	130.7	103.0, 84.2, 72.5, 71.3	27.1, 26.9, 18.2, 17.2	19.5 18.8	83.6	38.7	70.8	87.7	62.2
5b	150.3	152.7[d]	94.1	155.1[d]	130.6	103.2, 84.2, 72.6, 71.3	27.0, 26.9, 18.2, 17.2	19.5 18.7	83.8	38.7	70.3	85.5	64.0

[a] Measured in [D_6]DMSO at 298 K. [b] Purine numbering. [c] Systematic numbering. [d] Tentative.

stabilizing the ‘dG–dC’ base pair.[19–22,25] While 7-alkynyl chains with one triple bond and three to six carbon atoms led to stabilization of duplex DNA, longer chains are destabilizing due to the increased hydrophobic character.[19–22,25] Recently, we demonstrated that long chain linkers with two triple bonds like octadiynyl residues or propargyl ether moieties show a positive influence on the duplex stability similar to that of a propynyl residue.[14,27] The advantage of such linkers is the presence of the additional terminal triple bond which enhances the hydrophilic character of the linker. Water molecules can be bound to the side chain. We anticipate hydrogen bonding between water and triple bonds.

To evaluate the potential of the base modification on the duplex stability and fluorescence properties, oligonucleotides were prepared by solid-phase synthesis using the phosphoramidites **3a** and **3b** as well as standard building blocks. Their synthesis was performed in a 1 μmol scale employing phosphoramidite chemistry. The coupling yields were always higher than 95%. Deprotection of the oligomers was performed in 25% aqueous NH_3 at 60 °C for 18–24 h. The oligonucleotides were purified before and after detritylation by reversed-phase HPLC. The base composition of the oligonucleotides was determined by tandem enzymatic hydrolysis with snake-venom phosphodiesterase followed by alkaline phosphatase in 0.1 M Tris-HCl buffer (pH 8.5) at 37 °C (for details see experimental section). The homogeneity of the oligonucleotides was confirmed by MALDI-TOF mass spectrometry. The detected masses were in good agreement with the calculated values (Table 7).

Single and multiple incorporations of **2d**, replacing dG-residues within various positions of the reference duplex 5′-d(TAG GTC AAT ACT) (**6**) and 3′-d(ATC CAG TTA TGA) (**7**) were performed. As shown in Table 2, the replacements of dG by nucleoside

Table 2 T_m-values and thermodynamic data of oligonucleotide duplexes containing **1**, **2c** and **2d**[a]

Duplexes	T_m/°C	ΔT_m [b]/°C	ΔG°_{310} [c]/kcal mol^{-1}
5′-d(TAG GTC AAT ACT) (**6**)	50	—	−11.8
3′-d(ATC CAG TTA TGA) (**7**)	(47)	—	−10.9
5′-d(TAG GTC AAT ACT) (**6**)	53[18]	+3	−12.5
3′-d(ATC CA**2c** TTA TGA) (**8**)	(49)	+2	
5′-d(TA**2c 2c**TC AAT ACT) (**9**)	56[18]	+3	−14.5
3′-d(ATC CAG TTA TGA) (**7**)	(52)	+2.5	
5′-d(TA**2c 2c**TC AAT ACT) (**9**)	58[18]	+2.7	−14.0
3′-d(ATC CA**2c** TTA TGA) (**8**)	(56)	+3	
5′-d(TAG GTC AAT ACT) (**6**)	52[14]	+2	−11.8
3′-d(ATC CAG TTA T**1**A) (**10**)			
5′-d(TA**1 1**TC AAT ACT) (**11**)	53[14]	+1.5	−12.3
3′-d(ATC CAG TTA TGA) (**7**)			
5′-d(TA**1 1**TC AAT ACT) (**11**)	55[14]	+1.7	−12.7
3′-d(ATC CAG TTA T**1**A) (**10**)			
5′-d(TAG GTC AAT ACT) (**6**)	52	+2	−12.9
3′-d(ATC CA**2d** TTA TGA) (**12**)	(49)	+2	−11.7
5′-d(TAG GTC AAT ACT) (**6**)	53	+4	−14.2
3′-d(ATC CAG TTA T**2d**A) (**13**)			
5′-d(TA**2d 2d**TC AAT ACT) (**14**)	54	+2	−12.5
3′-d(ATC CAG TTA TGA) (**7**)			
5′-d(TA**2d 2d**TC AAT ACT) (**14**)	58	+2.7	−14.6
3′-d(ATC CAG TTA T**2d**A) (**13**)			
5′-d(TA**2d 2d**TC AAT ACT) (**14**)	60	+3.3	−15.0
3′-d(ATC CA**2d** TTA TGA) (**12**)	(54)	+2.3	−13.6

[a] Measured at 260 nm in 1 M NaCl, 100 mM $MgCl_2$, and 60 mM Na-cacodylate (pH 7.0) with 5 μM + 5 μM single-strand concentration. Data in parentheses were measured in 100 mM NaCl, 10 mM $MgCl_2$ and 10 mM Na-cacodylate (pH 7.0) at the same concentration. [b] Refers to the contribution of the modified residues divided by the number of replacements. [c] ΔG°_{310} values are given with 15% error.

2d result in a T_m increase of 2–3 °C per modification. These values are close to the T_m values found for oligonucleotide duplexes containing 8-aza-7-deaza-7-propynyl-dG (**2c**) or 7-deaza-7-octa-1,7-diynyl-dG (**1**) at identical positions with the tendency of duplex stabilization. Thus, the space demanding octadiynyl side chain has a positive influence on the DNA duplex stability as already observed for propynyl residues (**2c** = **2d** > **1**).

3. Functionalization of nucleosides and oligonucleotides with 3-azido-7-hydroxycoumarin (15) by the Huisgen-Meldal-Sharpless [2 + 3] cycloaddition

The dye functionalization of nucleoside **2d** as well as oligonucleotides 5′-d(AGT ATT **2d**AC CTA) (**12**) and 5′-d(A**2d**T ATT GAC CTA) (**13**) by the azide-alkyne 'click reaction' was performed. The octa-1,7-diynyl nucleoside **2d** with a terminal triple bond was functionalized with the non-fluorescent coumarin azide **15** in an ethanol–water mixture to form the 'click' adduct **16** in 90% yield when sodium ascorbate and $CuSO_4$ as a catalyst were used (Scheme 3). For details see the experimental section. The ^{13}C-NMR spectra show the absence of the terminal C≡C carbon atom signals, and the new appearing double bond signals of the 1,2,3-triazole moiety identified at δ = 122.9 ppm and δ = 146.8 ppm (Table 5). Due to steric hindrance, a bis-functionalization of the second triple bond is not observed.[23,24,28] The structure of the conjugate **16** was assigned on the basis of ^{13}C-NMR spectra and $J_{C,H}$ coupling constants (Table 5 and Table 6, see experimental section). The ^{13}C-NMR chemical shifts of the side chain for the dye conjugate **16** are almost identical to those of the 7-deaza-2′-deoxyguanosine coumarin conjugate **17** (Scheme 3). In both cases the $J_{C,H}$ coupling constants for triazole-C5, H-C5 are 199 Hz. Moreover, the resonance of the triazole ring carbons is clearly evidenced by ^{1}H-NMR, gated decoupled ^{1}H-^{13}C as well as DEPT-135 NMR spectroscopy.

The 7-octadiynyl side chain of compound **2d** has a strong influence on the UV spectrum of 8-aza-7-deaza-2′-deoxyguanosine. UV data are shown in Table 3 and spectra are given in Fig. 2. The short wavelength maximum of the alkynyl nucleoside is shifted hypsochromically from 254 to 243 nm compared to the non-functionalized compound **2a** or the iodo derivative **2b**. The UV spectra of the 'click' products **16** and **17** are a combination of the UV spectra of either compound **1** or **2d**, the coumarin azide **15** and the 1,2,3-triazole moiety (Fig. 2a). Thus, the conjugate can be easily identified by the long wavelength absorption maximum of coumarin moiety at 346 nm in methanol. This is also valid for oligonucleotides incorporating the dye conjugate **16** (356 nm in water).

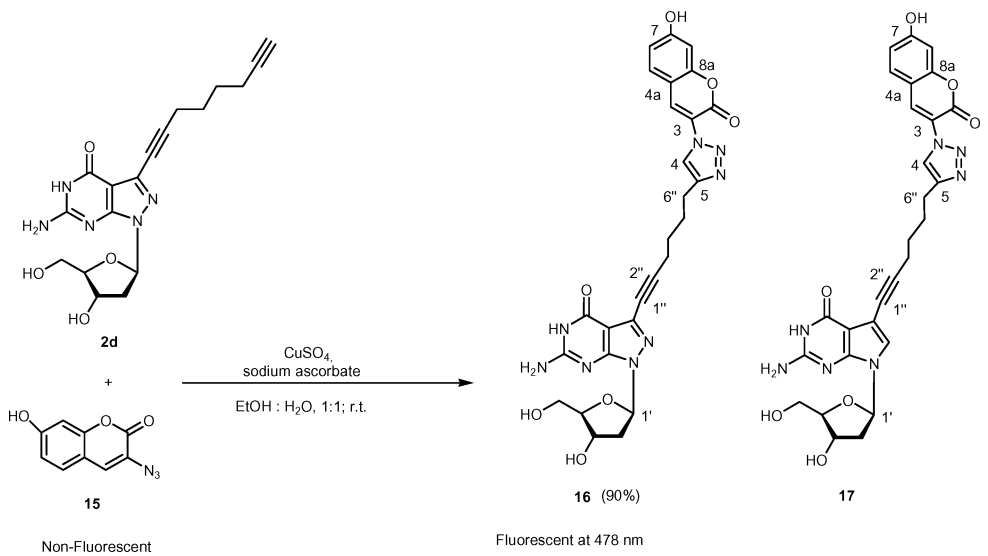

Scheme 3 Functionalization of nucleoside **2d** with 3-azido-7-hydroxycoumarin (**15**).

Table 3 UV maxima and molar absorptivity (mol. abs.) of compound **2d** and corresponding derivatives[a]

Cpd.	Wavelength (λ_{max})/nm	Mol. Abs. (ε)	Cpd.	Wavelength (λ_{max})/nm	Mol. Abs. (ε)
1[7]			**17**	220	26900
	240	20200		240 (sh)	19000
	273	9000		274	7200
	294	8100		298	7300
				346	13300
2a[26]	254	14200	**2b**[16]	258	10800
2c[18]	242	27300	**15**	342	12300
2d	243	28000	**16**	243	25200
				346	13200

[a] Measured in methanol.

Next, the cycloaddition 'click' reaction was performed on the oligonucleotide level using 5 A_{260} units of the purified oligonucleotides 5′-d(AGT ATT **2d**AC CTA) (**12**) and 5′-d(A**2d** T ATT GAC CTA) (**13**) each containing one 8-aza-7-deaza-7-(octa-1,7-diynyl)-2′-deoxyguanosine residue. Both oligonucleotides were separately functionalized with the non-fluorescent coumarin azide **15**.[29] The reaction was performed in aqueous solution (H_2O–*t*-BuOH–DMSO) in the presence of a complex of $CuSO_4$–TBTA (tris(benzyltriazoylmethyl)amine) (1 : 1), TCEP (tris(carboxyethyl)phosphine) and $NaHCO_3$ (Scheme 4). $NaHCO_3$ was essential for the completion of the reaction within 12 h yielding the strongly fluorescent oligonucleotides 5′-d(AGT ATT **16**AC CTA) (**18**) and 5′-d(A**16** T ATT GAC CTA) (**19**). For details see the experimental section. The oligonucleotides were purified by reversed-phase HPLC and characterized by MALDI-TOF mass spectra (Table 7), UV-spectroscopy (Fig. 2b) as well as by the HPLC elution profile (Scheme 4). The UV/VIS spectrum of oligonucleotide **19** shows two maxima which can be attributed to the absorption of the canonical nucleobases at 260 nm and the coumarin dye at 356 nm.

Composition analyses of the oligonucleotides **13** and **19** were performed using snake venom phosphodiesterase (*Crotallus adamanteus*, EC 3.1.15.1) and alkaline phosphatase (*E. coli*, EC 3.1.3.1).[14] The composition is shown in the HPLC profile of the digest demonstrating that all monomeric components including the modified nucleoside **2d** as well as the 'click' product **16** are not affected during oligonucleotide synthesis and conjugation. As expected, the lipophilicity of a compound increases by increasing the length of the side chain from the propynyl derivative **2c** to the octadiynyl compound **2d** as displayed by the reversed-phase HPLC profile (Figure S2, see supporting information). The introduction of the hydrophilic coumarin residue makes the conjugate less lipophilic than the starting material **2d**; thus the conjugate **16** is migrating faster than **2d**. The information obtained from the artificial nucleoside mixture was beneficial for the peak assignment of the enzymatic digest (Fig. 3).

4. Fluorescence properties of nucleoside and oligonucleotide 3-azido-7-hydroxycoumarin conjugates and DNA duplex stability

Pyrrolo[2,3-*d*]pyrimidine nucleoside dye conjugates show significantly lower fluorescence than those of pyrimidine nucleosides; a phenomenon which was studied with 7-hydroxycoumarin as reporter group.[14] Now the fluorescence properties of compound **16** were investigated and compared with those of **17** at pH 8.5. Under alkaline conditions (pH 8.5), the 7-hydroxycoumarin dye exists predominantly in the anionic form.[14,30] Both compounds show similar excitation maxima (398 nm for dye **16** *vs.* 393 nm for dye **17**) with emission maxima at 478 nm and 477 nm, respectively, both measured in 0.1 M Tris-HCl-buffer at pH 8.5 (Fig. 4a and b). For solubility reasons the coumarin 1,2,3-triazolyl conjugates **16** and **17** were dissolved in 0.5 ml of DMSO and then diluted with 99.5 ml 0.1 M Tris-HCl buffer, pH 8.5. In all experiments the concentration of the nucleoside dye conjugates was identical (9.4×10^{-3} mol l^{-1}).

From Fig. 4b, it is apparent that the 8-aza-7-deaza-2′-deoxyguanosine dye conjugate **16** develops a much stronger fluorescence than the conjugate **17** (Fig. 4a). This is clearly evidenced by their direct comparison in Fig. 4c showing that the fluorescence maximum of **16** is about 10-times higher than that of **17**. Next, the Cu(I)-catalyzed azide-alkyne cycloaddition of **1** and **2d** with non-fluorescent 3-azido-7-hydroxycoumarin (**15**) affording the nucleoside dye conjugates **17** and **16** was followed by fluorescence measurements (Fig. 4d). It is evident that during the formation of the pyrrolo[2,3-*d*]pyrimidine dye conjugate **17** only a small fluorescence increase is observed, whereas the formation of

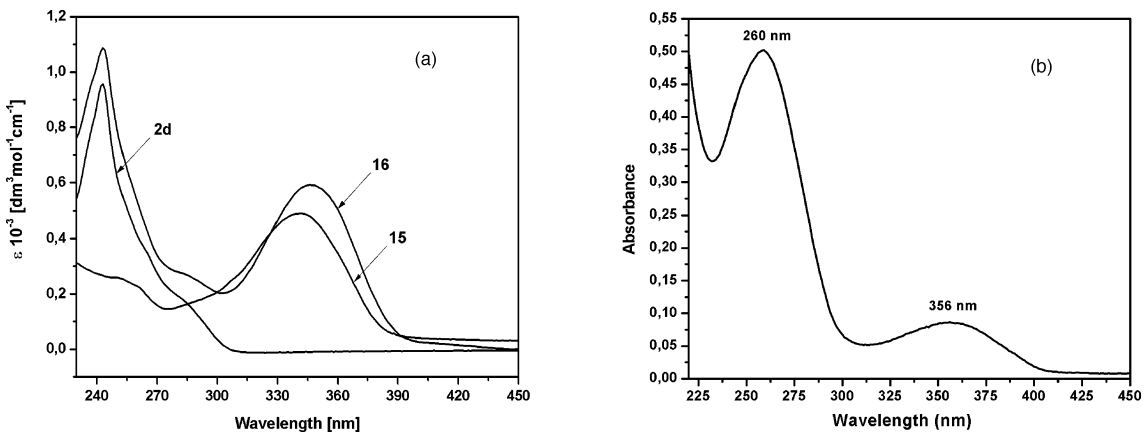

Fig. 2 (a) UV/VIS spectra of nucleoside **2d**, coumarin azide **15** and the coumarin conjugate **16** measured in methanol. (b) UV/VIS spectrum of the oligonucleotide coumarin conjugate 5′-d(A**16** T ATT GAC CTA) (**19**) measured in distilled water.

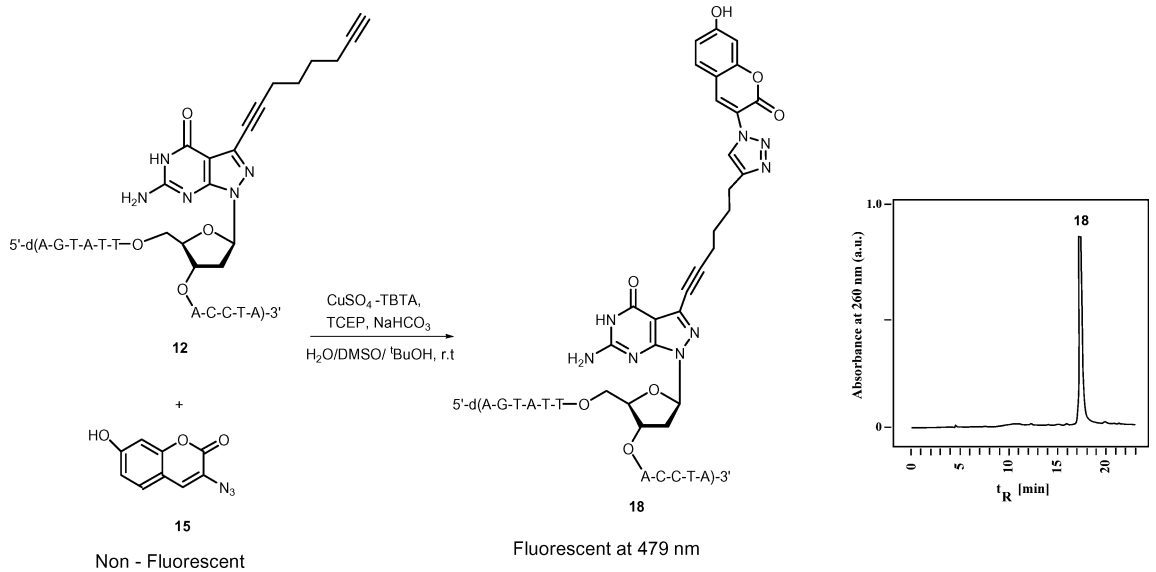

Scheme 4 Huisgen-Meldal-Sharpless [2 + 3] cycloaddition of oligonucleotide **12** incorporating nucleoside **2d** with 3-azido-7-hydroxycoumarin (**15**) and HPLC profile of oligonucleotide **18** on a RP-18 (250 × 4 mm) column at 260 nm. Gradient: 0–20 min 0–20% A in B, 20–30 min 20–30 A in B with a flow rate of 0.7 ml min^{-1}. Solvent systems: MeCN (A) and 0.1 M (Et_3NH)OAc (pH 7.0)–MeCN, 95 : 5 (B).

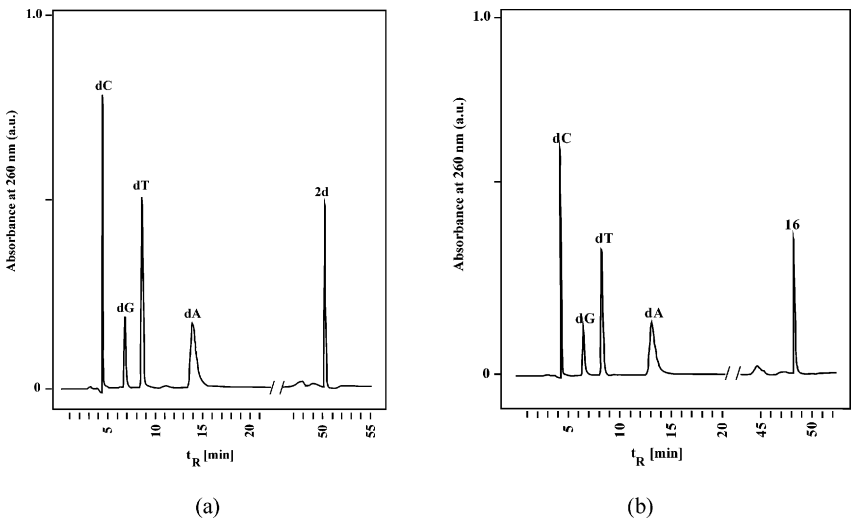

Fig. 3 HPLC profiles of the enzymatic hydrolysis products of (a) the oligonucleotide **13** and (b) the oligonucleotide **19** obtained after digestion with snake-venom phosphodiesterase and alkaline phosphatase in 0.1 M Tris-HCl buffer (pH 8.5) at 37 °C. Gradient: 0–25 min 100% B, 25–60 min 0–50% A in B; flow rate 0.7 ml min^{-1}. The following solvent systems were used: MeCN (A) and 0.1 M (Et_3NH)OAc (pH 7.0)–MeCN, 95 : 5 (B).

the pyrazolo[3,4-*d*]pyrimidine dye conjugate **16** leads to a much stronger increase of fluorescence.

Next, the fluorescence properties were studied on the oligonucleotides **18** and **19** containing the 1,2,3-triazole coumarin derivative **16** as monomeric building block. The fluorescence spectra of both single-stranded oligonucleotides **18** and **19** show a strong fluorescence with emission maxima at 479 nm and excitation maxima at 401 nm (Fig. 5a and c). Upon hybridization with the non-modified complementary strands the duplexes 5′-d(TAG GTC AAT ACT) (**6**) · 3′-d(ATC CAG TTA T**16**A) (**19**) and 5′-d(TAG GTC AAT ACT) (**6**) · 3′-d(ATC CA**16** TTA TGA) (**18**) are formed where **16** is located either near the 5′-terminus (Fig. 5b) or in a central position (Fig. 5d). No significant fluorescence change is observed during duplex formation resulting in almost identical fluorescence intensities of single-stranded and duplex DNA. This observation is contrary to that of the related oligonucleotide pyrrolo[2,3-*d*]pyrimidine nucleoside coumarin conjugate **17**. Here, a strong fluorescence decrease (85%) for the coumarin dye was found upon duplex formation.[14]

The single-stranded oligonucleotide 5′-d(A**16** T ATT GAC CTA) (**19**) containing the 8-aza-7-deaza-2′-deoxyguanosine dye conjugate **16** was then subjected to enzymatic phosphodiester hydrolysis by snake venom phosphodiesterase (0.1 M Tris-HCl buffer, pH 8.5). The fluorescence was measured at 479 nm with a fixed excitation wavelength (396 nm). Within 20 min, a fluorescence increase for oligonucleotide **19** by a factor of 3.4 was observed (Fig. 6a). Dephosphorylation with alkaline phosphatase (incubation at 37 °C for 9 h) did not lead to

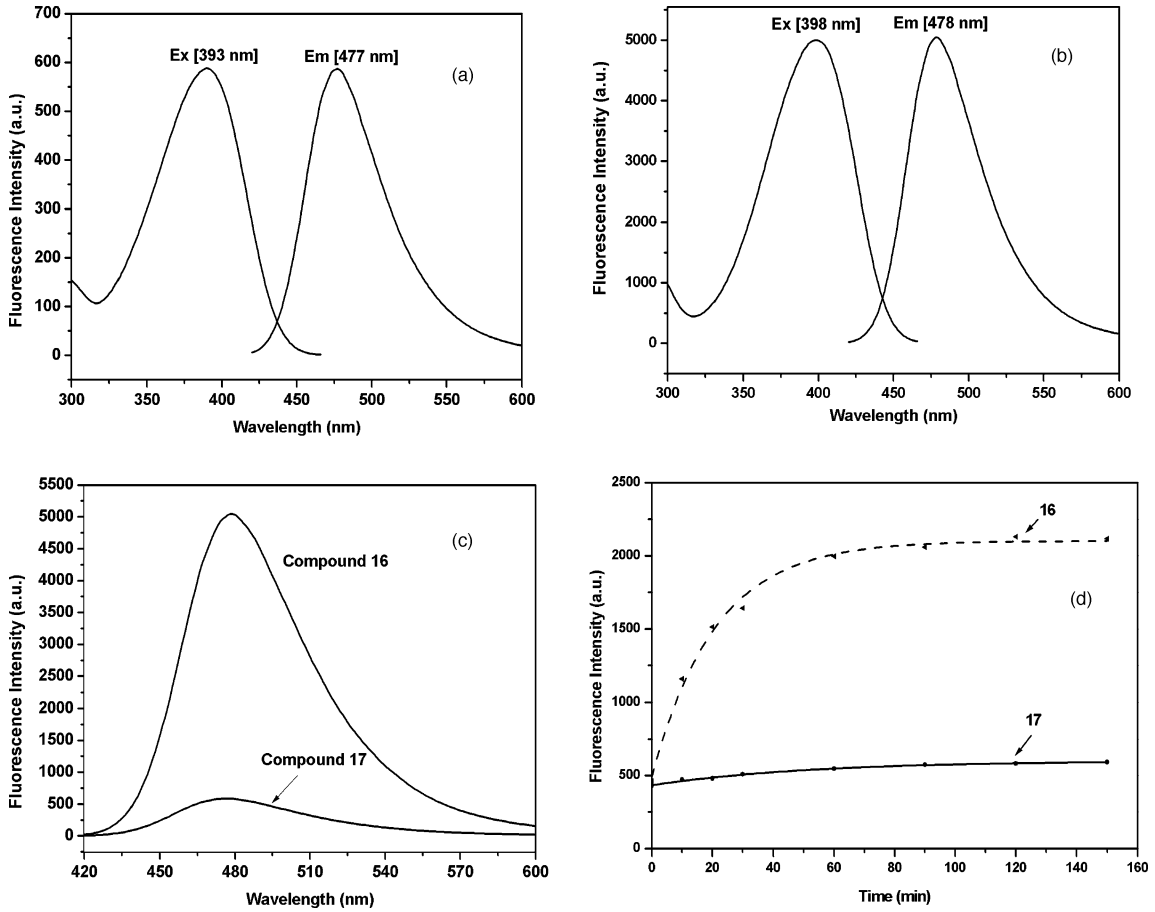

Fig. 4 The excitation and emission spectra of (a) the octa-1,7-diynylated pyrrolo nucleoside coumarin conjugate **17** and (b) the octa-1,7-diynylated pyrazolo nucleoside coumarin conjugate **16**. (c) The direct comparison of the emission spectra of the coumarin dye conjugates **16** and **17**. All spectra were measured in a mixture of DMSO (0.5 ml) and 99.5 ml of 0.1 M Tris-HCl buffer at pH 8.5 with a concentration of 9.4×10^{-3} mol l^{-1}. (d) Time dependent fluorescence increase during the Cu(I)-catalyzed azide-alkyne cycloaddition of **1** and **2d** with 3-azido-7-hydroxycoumarin (**15**). The reaction was performed in THF : *t*-BuOH : H_2O (3 : 1 : 1) at 12.5 mM nucleoside concentration with 30 mM dye concentration and 100 mM Na-ascorbate (pH 8.5). The reaction was started with aq. $CuSO_4$ (25 mM final concentration).

a further fluorescence change. When these experiments were performed with the oligonucleotide 5′-d(A**17** T ATT GAC CTA) (**20**) incorporating the 7-deaza-2′-deoxyguanosine dye conjugate **17**, a completely different observation was made. The hydrolysis of oligonucleotide **20** incorporating the 7-deaza-2′-deoxyguanosine dye conjugate **17** resulted in a strong fluorescence quenching (Fig. 6b).

The fluorescence phenomena observed on the nucleoside coumarin dye conjugates **16** and **17** as well as on the oligonucleotides **19** and **20** incorporating **16** and **17** need justification. Static and dynamic fluorescence quenching of coumarins by nucleobase derivatives has already been reported.[31–33] Nucleobase-specific quenching by fluorescence resonance transfer can be ruled out by the lack of appropriate spectral properties.[31] Therefore, it becomes likely, that photoinduced electron transfer and proton coupled electron transfer have to be considered. The redox properties of nucleobases, nucleosides and coumarin derivatives were already reported by Seidel *et al.*[31] A correlation of dye quenching and the oxidation potential of nucleobases was made. Intermolecular quenching experiments with different dyes and DNA constituents (conjugates) were performed. The data give evidence for the formation of non-fluorescent ground state complexes between the dye and the nucleobases. Only upon contact formation, efficient fluorescence quenching occurs *via* electron transfer. Considering these findings and adopting this to the pyrrolo[2,3-*d*]pyrimidine and pyrazolo[3,4-*d*]pyrimidine coumarin dye conjugates, it is evident that the stronger electron-donating 7-deaza-2′-deoxyguanosine conjugate (**17**) is a better quencher for the coumarin moiety than the dye conjugate of 8-aza-7-deaza-2′-deoxyguanosine (**16**). When the conjugate **17** serves as constituent of oligonucleotides the 7-deaza-2′-deoxyguanosine moiety participates in base stacking. Almost no contact formation between the base and the coumarin moiety is possible thereby preventing fluorescence quenching. The fluorescence decreases upon phosphodiester hydrolysis (monomeric conjugate formation) due to formation of a contact complex between the nucleobase and the dye; either in an intramolecular or intermolecular way. Nevertheless, the opposite behavior—increase of the fluorescence—of the 8-aza-7-deaza-2′-deoxyguanosine coumarin conjugate **16** is observed when it is released from the oligonucleotide **19**. Here, the oxidation potential of the pyrazolo[3,4-*d*]pyrimidine moiety is too high to transfer an electron to the coumarin dye (negligible

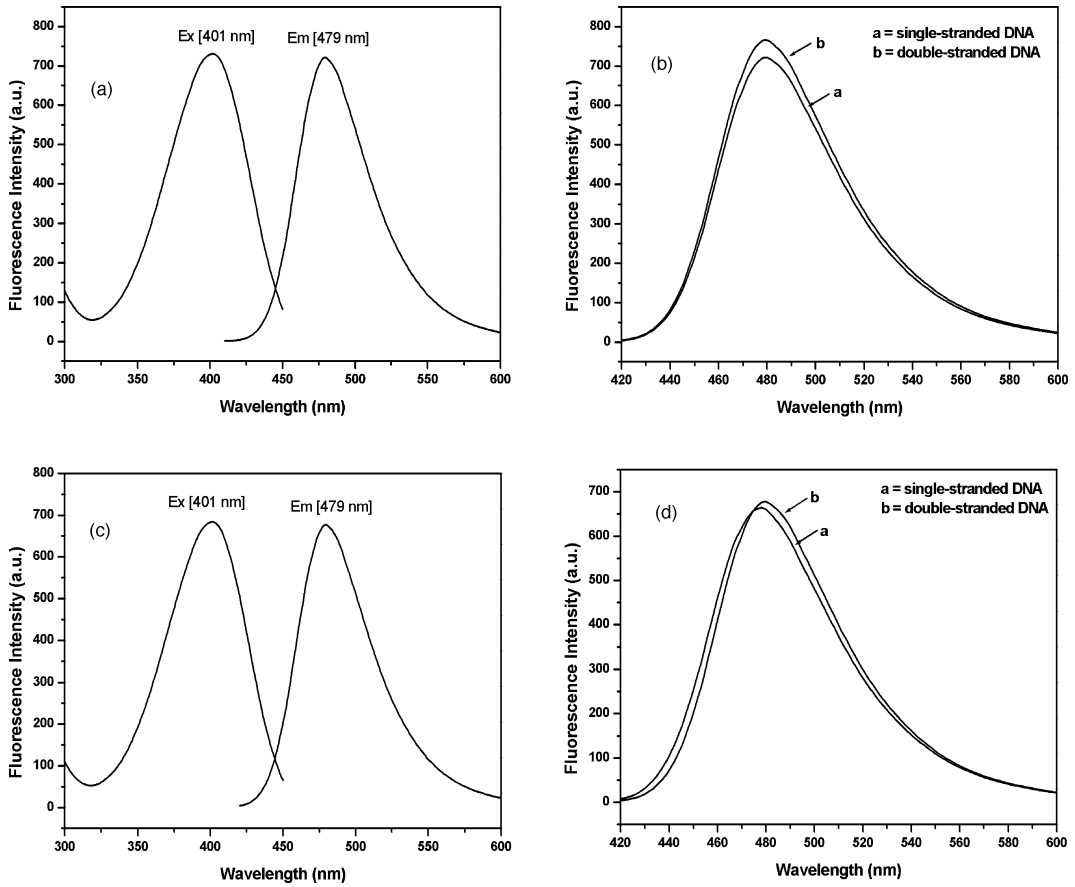

Fig. 5 (a) The excitation and emission spectra of the single-stranded oligonucleotide **19** (2 μM single-strand concentration); (b) comparison of the fluorescence emission spectra of the single-stranded oligonucleotide **19** and the duplex **19** · **6** (2 μM + 2 μM single-strand concentration) when excited at 401 nm; (c) the excitation and emission spectra of the single-stranded oligonucleotide **18** (2 μM single-strand concentration); (d) comparison of the fluorescence emission spectra of the single-stranded oligonucleotide **18** and the duplex **18** · **6** (2 μM + 2 μM single-strand concentration) when excited at 401 nm. All spectra were measured in 1 M NaCl, 100 mM $MgCl_2$, 60 mM Na-cacodylate buffer at pH = 8.5.

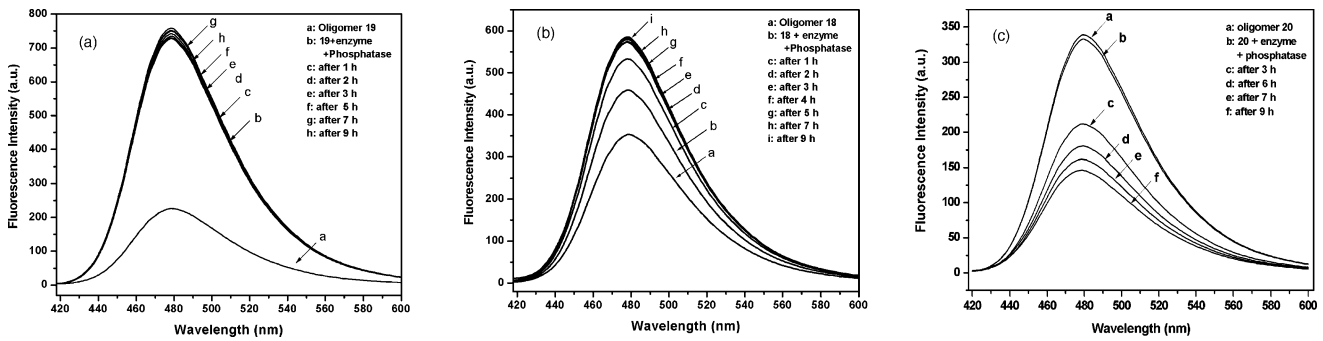

Fig. 6 Fluorescence spectra obtained after the enzymatic digestion of (a) 1.8 μM of the single-stranded oligonucleotide 5′-d(A**16** T ATT GAC CTA) (**19**), (b) 2.3 μM of the single-stranded oligonucleotide 5′-d(AGT ATT **16**AC CTA) (**18**) and (c) 1.7 μM of the single-stranded oligonucleotide 5′-d(A**17** T ATT GAC CTA) (**20**) with snake venom phosphodiesterase and alkaline phosphatase in 1 ml of 0.1 M Tris-HCl buffer (pH 8.5) at 37 °C.[14]

quenching). However, a hyperchromic effect is existing when the dye conjugate is integrated into the oligonucleotide chain. This can cause a hyperchromic change after enzymatic digestion.

To evaluate the influence of dye modification on the duplex stability, the T_m values of the reference oligonucleotide duplex 5′-d(TAG GTC AAT ACT) (**6**) and 3′-d(ATC CAG TTA TGA) (**7**) modified by the octadiynylated side chain derivative **2d** or the dye conjugate **16** were measured. The replacement of one dG residue at the periphery of the duplex **6** · **7** by nucleoside **2d** (**6** · **13**) resulted in a T_m increase of 3 °C (Table 4). Replacement of a dG-residue within the central position of the duplex (**6** · **12**) led to a T_m increase of 2 °C. However, the effect of the nucleoside coumarin conjugates **16** or **17** on the duplex stability is not clear. The introduction of **16** in duplex **6** · **19** has almost no effect on the duplex stability (ΔT_m = +3 °C) compared to the corresponding octadiynylated duplex (**6** · **13**) while for duplex **6** · **18** containing **16** and for duplex

Table 4 T_m-Values of oligonucleotide duplexes containing 8-aza-7-deaza-2′-deoxyguanosine derivatives

Duplex	T_m [a]/ °C	ΔT_m [b]/ °C	T_m [c]/ °C	ΔT_m [b]/ °C
5′-d(TAG GTC AAT ACT) (**6**) 3′-d(ATC CAG TTA TGA) (**7**)	50	—	47	—
5′-d(TA**2a2a**TC AAT ACT) (**21**) 3′-d(ATC CA**2a** TTA T**2a**A) (**22**)	50*[21]	0	—	—
5′-d(TAG GTC AAT ACT) (**6**) 3′-d(ATC CA**2d** TTA TGA) (**12**)	52*	+2	48	+1
5′-d(TAG GTC AAT ACT) (**6**) 3′-d(ATC CAG TTA T**2d**A) (**13**)	53	+3	52	+5
5′-d(TAG GTC AAT ACT) (**6**) 3′-d(ATC CA**16** TTA TGA) (**18**)	47	−3	49	+2
5′-d(TAG GTC AAT ACT) (**6**) 3′-d(ATC CAG TTA T**16**A) (**19**)	53	+3	53	+6
5′-d(TAG GTC AAT ACT) (**6**) 3′-d(ATC CAG TTA T**1**A) (**21**)	52[14]	+2	—	—
5′-d(TAG GTC AAT ACT) (**6**) 3′-d(ATC CAG TTA T**17**A) (**20**)	47	−3	—	—

[a] Measured at 260 nm in 1 M NaCl, 100 mM $MgCl_2$, and 60 mM Na-cacodylate (pH 7.0) with 2 μM + 2 μM single-strand concentration. [b] Refers to the contribution of the modified residues divided by the number of replacements. [c] Measured at 260 nm in 1 M NaCl, 100 mM $MgCl_2$, and 60 mM Na-cacodylate (pH 8.5) with 2 μM + 2 μM single-strand concentration. T_m values marked with an asterisk were measured at a 5 μM + 5 μM single-strand concentration.

6 · **20** containing **17** a strong destabilization was observed (ΔT_m = −3 °C). A destabilizing interaction of the coumarin moiety with the duplex helix has to be considered.

For comparison, the duplex stabilities of **6** · **19** and **6** · **18** were determined at pH 8.5; a pH value at which coumarin forms an anionic species. Under these conditions a much stronger stabilization of **6** · **19** compared to the reference duplex **6** · **7** was observed (ΔT_m = +6 °C). Moreover, duplex **6** · **18** which was destabilized at pH 7 (ΔT_m = −6 °C) shows a T_m increase (ΔT_m = +2 °C) under alkaline conditions (pH 8.5). As the coumarin dye is negatively charged at pH = 8.5, ionic interaction with the phosphodiester backbone can be excluded and the coumarin dye is protruding into the major groove of B-DNA. This favourable behaviour is supported by earlier data obtained on 2′-deoxypseudourine dye conjugates bearing negative charges.[34] In contrast, positively charged dyes showed a tendency to interact with the negatively charged phosphodiester backbone supported by significant differences in the melting behaviour.

Next, molecular dynamics simulations using Amber MM+ force field (Hyperchem 7.0/8.0; Hypercube Inc., Gainesville, FL, USA, 2001) were performed on the 12-mer duplexes **6** · **12** and **6** · **18**. The energy minimized molecular structures are built as B-type DNA and are shown in Fig. 7. Fig. 7a displays a duplex (**6** · **12**) in which a central dG-residue is replaced by the octa-1,7-diynyl derivative of 8-aza-7-deaza-2′-deoxyguanosine (**2d**). According to Fig. 7a, the alkynyl group linked to the pyrazolo[3,4-*d*]pyrimidine base is linear and in plane with the heterocyclic base as it was observed earlier by the X-ray structure of the related molecule 7-deaza-7-propynyl-2′-deoxyguanosine (**1c**).[35] Moreover, the duplex structure is not disturbed by the modification.

In Fig. 7b and Fig. 7c, the energy minimized model of the oligonucleotide duplex containing the coumarin conjugate **16** is shown by two different views. Also in this case the bulky residue is well accommodated in the major groove of DNA. The triazole moiety does not develop stacking interaction with the base pairs of the duplex and seems to have steric freedom not disturbing the B-DNA duplex.

Conclusion and outlook

8-Aza-7-deaza-7-octa-1,7-diynyl-2′-deoxyguanosine (**2d**) was synthesized by the *Sonogashira* cross-coupling reaction from 8-aza-7-deaza-7-iodo-2′-deoxyguanosine (**2b**) and excess octadiyne. Nucleoside **2d** was converted into phosphoramidite building blocks (**3a**, **b**) and oligonucleotides were prepared. The replacement of dG residues by the 7-octadiynyl nucleoside **2d** increases the dG-dC base pair stability in a similar way as 8-aza-7-deaza-7-propynyl-2′-deoxyguanosine (**2c**) and 7-deaza-7-octa-1,7-diynyl-2′-deoxyguanosine (**1**). The octa-1,7-diynylated pyrazolo[3,4-*d*]pyrimidine derivative **2d** bearing a partially stiff linker arm and a terminal triple bond was further functionalized by the

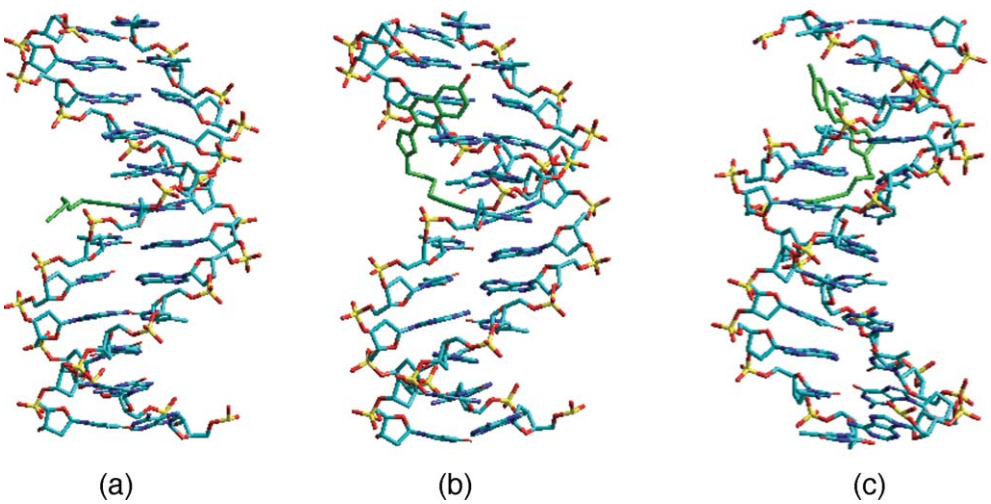

Fig. 7 Molecular models (a) of duplex 5′-d(TAG GTC AATACT) (**6**) · 3′-d(ATC CA**2d** TTA TGA) (**12**), (b) and (c) duplex 5′-d(TAG GTC AAT ACT) (**6**) · 3′-d(ATC CA**16** TTA TGA) (**18**). The models were constructed using Hyperchem 7.0/8.0 and energy minimized using the AMBER calculations.

azide-alkyne *Huisgen-Meldal-Sharpless* cycloaddition ('click' reaction) on the stages of nucleosides and oligonucleotides.

The conjugation of the terminal triple bond with the non-fluorescent 3-azido-7-hydroxycoumarin **15** resulted in the formation of highly fluorescent dye conjugates. The fluorescence intensity of the 8-aza-7-deaza-2′-deoxyguanosine conjugate **16** was found to be about ten times higher than of the corresponding 7-deaza-2′-deoxyguanosine conjugate **17**. The quenching induced by the pyrrolo[2,3-*d*]pyrimidine base on the coumarin dye vanishes in the case of the pyrazolo[3,4-*d*]pyrimidine conjugate. According to our data[14] and the observation by others,[31,36,37] an electron transfer from the pyrrolo[2,3-*d*]pyrimidine nucleobase to the dye is suggested which is not occuring in the case of pyrazolo[3,4-*d*]pyrimidines. Fig. 8 displays possible intramolecular contact complexes within one nucleoside dye conjugate (a, b) and intermolecular contact complexes between two nucleoside dye conjugates.

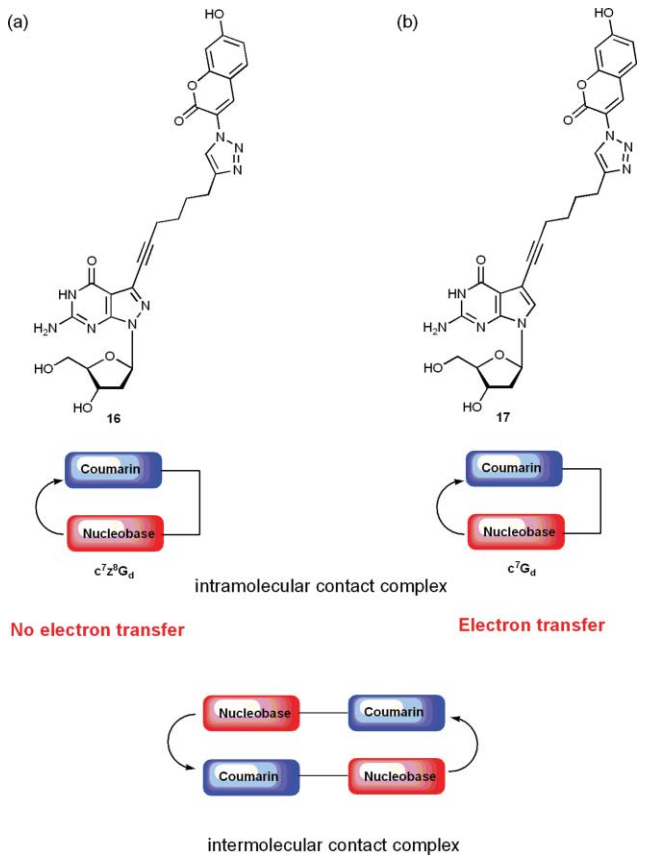

Fig. 8 Intramolecular and intermolecular contact complexes within nucleoside dye conjugates.

8-Aza-7-deaza-2′-deoxyguanosine and 7-deaza-2′-deoxyguanosine are the most ideal shape mimics of 2′-deoxyguanosine allowing functionalization at the 7-position not disturbing the DNA helix structure. Their coumarin conjugates (**16** and **17**) show almost identical base pairing properties but strong differences in their fluorescence intensity. The differences of nucleobase specific quenching has the potential to be applied in DNA and RNA detection or sequencing.[38,39]

Table 5 ^{13}C-NMR chemical shifts of the nucleoside coumarin conjugates **16** and **17**

Cpd.	C(2) [b]C(6)[c]	C(4) [b]C(7a)[c]	C(5) [b]C(3a)[c]	C(6) [b]C(4)[c]	C(7) [b]C(3)[c]
17	154.6	150.1[d]	99.5	157.9[d]	89.7
16	156.4	155.3[d]	93.3	156.9[d]	130.7
Cpd.	C(1′)	C(2′)	C(3′)	C(4′)	C(5′)
17	82.2	38.7	70.9	87.1	61.9
16	83.1	38.7	70.9	87.5	62.4
Cpd.	C≡C	Triazole	Coumarin		
17	101.0, 74.7	147.0, 122.9	162.3, 119.5, 136.1, 110.4, 130.8, 114.2, 156.4, 102.1, 154.6		
16	100.0, 73.2	146.8, 122.9	162.9, 119.2, 136.2, 110.1, 130.4, 114.4, 155.4, 102.2, 154.6		

[a] Measured in [D$_6$]DMSO at 298 K. [b] Purine numbering. [c] Systematic numbering. [d] Tentative.

Experimental

General

All chemicals were purchased from Acros, Fluka, or Sigma-Aldrich (Sigma-Aldrich Chemie GmbH, Deisenhofen, Germany). Solvents were of laboratory grade. Thin layer Chromatography (TLC): aluminium sheets, silica gel 60 F254 (0.2 mm; Merck, Darmstadt, Germany). Flash column chromatography (FC): silica gel 60 (VWR, Germany) at 0.4 bar; sample collection with an Ultra Rac II fractions collector (LKB Instruments, Sweden). UV spectra: U-3200 spectrometer (Hitachi, Tokyo, Japan); Reversed-phase HPLC was carried out on a 250 × 4 mm PR-18 column (Merck) with a Merck-Hitachi HPLC pump (model L-7100) connected with a variable wavelength monitor (model L-7400). NMR spectra: Avance-DPX-300 spectrometer (Bruker, Rheinstetten, Germany), at 300 MHz for ^{1}H and ^{13}C; δ in ppm relative to Me_4Si as internal standard or external 85% H_3PO_4 for ^{31}P. The J values are given in Hz. MALDI-TOF mass spectra were recorded with Applied Biosystems Voyager DE PRO spectrometer with 3-hydroxypicolinic acid (3-HPA) as a matrix. Elemental analyses were performed by Mikroanalytisches Laboratorium Beller (Göttingen, Germany). The melting temperature curves were measured with a Cary-100 Bio UV-VIS spectrophotometer (Varian, Australia) equipped with a Cary thermoelectrical controller. The temperature was measured continuously in the reference cell with a Pt-100 resistor, and the thermodynamic data of duplex formation were calculated by the MeltWin (version 3.0) program using the curve fitting of the melting profiles according to a two-state model.[40]

The fluorescence measurements were performed in bidistilled water at 20 °C. Fluorescence spectra were recorded in the wavelength range between 320 to 600 nm using the fluorescence spectrophotometer F-250 (Hitachi, Tokyo, Japan).

Synthesis, purification, and characterization of the oligonucleotides 6–14

The syntheses of oligonucleotides were performed on a DNA synthesizer, model 392–08 (Applied Biosystems, Weiterstadt, Gemany) at 1 µmol scale using the phosphoramidites

Table 6 Coupling constants J(C,H) [Hz] of 8-aza-7-deaza-2′-deoxyguanosine and 7-deaza-2′-deoxyguanosine derivatives[a,b]

	Coupling	J/Hz		
		2d	**17**	**16**
C1″≡	^3J(C1″, H-C3″)	3.6	—	5.6
C3″[c]	^1J(C3″, H-C3″)	130.0	145	132.0
	^2J(C3″, H-C4″)	5.4		
C4″	^1J(C4″, H-C4″)	69.6	—	—
C5″	^1J(C5″, H-C5″)	57.7	—	—
C6″[c]	^1J(C6″, H-C6″)	129.0	127.7	128.5
	^2J(C6″, H-C5″)	5.0		
C7″≡	^2J(C7″, H-C8″)	4.2	—	—
≡C8″	^1J(C8″, H-C8″)	248.0	—	—
	^3J(C8″, H-C6″)	4.2		
Triazole-C5	^1J(triazole-C5, H-C5)	—	198.9	199.0
Coumarin-C4	^1J(coumarin-C4, H-C4)	—	168.5	168.4
Coumarin-C5	^1J(coumarin-C5, H-C5)	—	168.7	164.9
Coumarin-C6	^1J(coumarin-C6, H-C6)	—	162.9	158.6
Coumarin-C7	^1J(coumarin-C7, H-C7)	—	120.0	114.3
Coumarin-C8	^1J(coumarin-C8, H-C8)	—	164.3	163.7
C1′	^1J(C1′, H-C1′)	160	163	163
C3′	^1J(C3′, H-C3′)	149	156	151
C4′	^1J(C4′, H-C4′)	149	148	147
C5′	^1J(C5′, H-C5′)	140	140	142

[a] Measured in [d_6]DMSO at 298 K. [b] Purine numbering. [c] Tentative.

3a and **3b** following the synthesis protocol for 3′-*O*-(2-cyanoethyl)phosphoramidites. After cleavage from the solid support, the oligonucleotides were deprotected in 25% aqueous ammonia solution for 12–16 h at 60 °C; The purification of the 'trityl-on' oligonucleotides was carried out on reversed-phase HPLC (Merck-Hitachi-HPLC; RP-18 column; gradient system (A = MeCN, B = 0.1 M (Et_3NH)OAc(pH 7.0)–MeCN, 95 : 5): 3 min 15% A in B, 12 min 15–50% A in B, and 5 min 50–10% A in B; flow rate 1.0 cm^3 min^{-1}. The purified 'trityl-on' oligonucleotides were treated with 2.5% $CHCl_2COOH$–CH_2Cl_2 for 5 min at 0 °C to remove the 4,4′-dimethoxytrityl residues. The detritylated oligomers were purified again by reversed-phase HPLC (gradient: 0–25 min 0–20% A in B; flow rate 1.0 ml min^{-1}). The oligomers were desalted on a short column (RP-18, silica gel) and lyophilized on a Speed-Vac evaporator to yield colorless solids which were frozen at –24 °C.

The enzymatic hydrolysis of oligonucleotide **13** and **19** was performed as described before using snake-venom phosphodiesterase (EC 3.1.15.1, *Crotallus adamanteus*) and alkaline phosphatase (EC 3.1.3.1, *Escherichia coli* from Roche Diagnostics GmbH, Germany) in 0.1 M Tris · HCl buffer (pH 8.5) at 37 °C, which was analyzed by reversed-phase HPLC (RP-18, 260 nm) showing the peaks of the modified and unmodified nucleosides.[14]

The synthesis of the oligonucleotide dye conjugates **18** and **19** was performed in aqueous solution with the non-fluorescent 3-azido-7-hydroxycoumarin **15** by the azide-alkyne 'click' reaction. The molecular masses of the oligonucleotides **6–14** and **18**, **19** were determined by MALDI-TOF mass spectrometry in the linear negative mode (see Table 7).

For the fluorescence quenching experiments, the enzymatic hydrolysis was performed using 1.7 μM single-stranded oligonucleotides dissolved in 1 cm^3 of 0.1 M Tris-HCl buffer (pH 8.5). To this solution, 0.005–0.010 cm^3 of snake venom phosphodiesterase and 0.005–0.010 cm^3 alkaline phosphatase were added and the fluorescence spectra were measured at different time intervals with an emission at 478 nm.

Table 7 Molecular mass [M – H]$^-$ of selected oligonucleotides determined by MALDI-TOF mass spectrometry

Oligonucleotides	[M – H]$^-$ (calc.)	[M – H]$^-$ (found)
5′-d(AGT ATT **2d**AC CTA) (**12**)	3748.6	3746.9
5′-d(TA**2d 2d**TC AAT ACT) (**14**)	3853.7	3849.7
5′-d(A**2d**T ATT GAC CTA) (**13**)	3745.7	3746.3
5′-d(AGT ATT **16**AC CTA) (**18**)	3948.8	3951.1
5′-d(A**16**T ATT GAC CTA) (**19**)	3948.8	3950.0
5′-d(A**17**T ATT GAC CTA)[14] (**20**)	3950.2[a]	3950.3[a]

[a] Determined as [M + H]$^+$ in the linear positive mode.

6-Amino-1-(2-deoxy-β-D-*erythro*-pentofuranosyl)-1,5-dihydro-3-(octa-1,7-diynyl)-4*H*-pyrazolo[3,4-*d*]pyrimidin-4-one (2d)

A solution of **2b** (1.0 g, 2.55 mmol) in dry DMF (5 cm^3) was treated with CuI (50 mg, 0.25 mmol), [Pd(PPh_3)$_4$] (150 mg, 0.125 mmol), dry Et_3N (0.5 cm^3, 0.25 mmol) and 5 equiv. of octa-1,7-diyne (12.75 mmol). The reaction mixture which slowly became black was stirred under N_2 for 12 h (TLC monitoring). Then, the mixture was diluted with MeOH–CH_2Cl_2 (1: 1, 25 cm^3), and Dowex HCO_3^- form (100 ± 200 mesh; 1.5 g) was added. After stirring for 15 min, the evolution of gas ceased. Stirring was continued for another 30 min, the resin was filtered off and washed with MeOH–CH_2Cl_2 (1 : 1, 250 cm^3). The combined filtrate was evaporated and the oily residue was adsorbed on silica gel and loaded on the top of a column. FC (silica gel, column 15 × 3 cm, eluted with CH_2Cl_2–MeOH 95 : 5 → 90 : 10 → 85 : 15) afforded one main zone. Evaporation of the solvent gave **2d** as colourless solid (500 mg, 52%) (Found: C, 57.98; H, 5.82; N, 18.57%. $C_{18}H_{21}N_5O_4$ requires C, 58.21; H, 5.70; N, 18.86%); TLC (silica gel, CH_2Cl_2–MeOH, 9 : 1): R_f 0.4; λ_{max} (MeOH)/nm 243 (ε/dm^3 mol^{-1} cm^{-1} 28 000); δ_H(250 MHz; [d_6]DMSO; Me_4Si) 1.64 (4 H, t, J 1.5, 2 × CH_2), 2.13 (1 H, m, 2′-H_α), 2.19 (2 H, m, C≡C-CH_2), 2.50 (2 H, t, J 6.5, C≡C-CH_2), 2.68 (1 H, m, 2′-H_β), 2.80 (1 H, t, J 2.4 Hz, C≡CH), 3.50 (2 H, m, 5′-H), 3.78 (1 H, t, J 2.9, 4′-H), 4.38 (1 H, m, 3′-H), 4.76 (1 H, t, J 5.4, 5′-OH), 5.25 (1 H, m, 3′-OH), 6.30 (1H, t, J 6.0, 1′-H), 6.75 (2 H, s, NH_2) and 10.70 (1 H, s, NH).

1-(2-Deoxy-*β*-D-*erythro*-pentofuranosyl)-6-{[(dimethylamino)methylidene]amino}-1,5-dihydro-3-(octa-1,7-diynyl)-4*H*-pyrazolo[3,4-*d*]pyrimidin-4-one (4a)

To a solution of **2d** (200 mg, 0.54 mmol) in MeOH (10 cm^3) was added *N*,*N*-dimethylformamide dimethyl acetal (1.5 cm^3). The reaction mixture was stirred for 2 h at rt, the solvent was evaporated and the oily residue was adsorbed on silica gel (50 g) and applied to FC (silica gel, column 10 × 4 cm, eluted with CH_2Cl_2–MeOH 95 : 5 → 90 : 10). Evaporation of the main zone afforded compound **4a** as colourless solid (202 mg, 88%) (Found: C, 59.12; H, 6.01; N, 19.60%. $C_{21}H_{26}N_6O_4$ requires C, 59.14; H, 6.14; N, 19.71%); TLC (silica gel, CH_2Cl_2–MeOH, 9 : 1): R_f 0.6; λ_{max} (MeOH)/nm 260 (ε/dm^3 mol^{-1} cm^{-1} 29 300), 300 (26 100); δ_H(250 MHz; [d_6]DMSO; Me_4Si) 1.64 (4 H, m, 2 × CH_2), 2.22 (1 H, m, 2′-H_α), 2.49 (4 H, m, 2 × C≡-CH_2), 2.65 (1 H, m, 2′-H_β), 2.77 (1 H, t, J 2.3, C≡CH), 3.05 (3 H, s, NCH_3), 3.19 (3 H, s,

NCH_3), 3.43 (2 H, m, 5′-H), 3.78 (1 H, m, 4′-H), 4.39 (1 H, m, 3′-H), 4.74 (1 H, t, *J* 5.6, 5′-OH), 5.25 (1 H, d, *J* 4.2, 3′-OH), 6.44 (1 H, t, *J* 6.4, 1′H), 8.67 (1 H, s, N=CH) and 11.31 (1 H, s, NH).

1-(2-Deoxy-5-*O*-(4,4′-dimethoxytriphenylmethyl)-*β*-D-*erythro*-pentofuranosyl)-6-{[(dimethylamino)methylidene]amino}-1,5-dihydro-3-(octa-1,7-diynyl)-4*H*-pyrazolo[3,4-*d*]pyrimidin-4-one (5a)

Compound **4a** (140 mg, 0.33 mmol) was dried by repeated co-evaporation with dry pyridine (3 × 5 cm^3). The residue was dissolved in dry pyridine and stirred with 4,4′-dimethoxytrityl chloride (200 mg, 0.64 mmol) in the presence of $(i\text{-Pr})_2EtN$ (0.1 cm^3, 0.58 mmol) at rt for 12 h. The solution was poured into 5% $NaHCO_3$ soln. and extracted with CH_2Cl_2 (3 × 30 cm^3). The combined extracts were dried (Na_2SO_4) and the solvent was evaporated. The residual foam was subjected to FC (silica gel, column 10 × 4 cm, eluted with CH_2Cl_2–acetone 95 : 5 → 90 : 10). Evaporation of the main zone afforded compound **5a** as colourless foam (184 mg, 77%) (Found: C, 69.02; H, 6.10; N, 11.42%. $C_{42}H_{44}N_6O_6$ requires C, 69.21; H, 6.08; N, 11.53%); TLC (silica gel, CH_2Cl_2–acetone 9 : 1): R_f 0.6; λ_{max} (MeOH)/nm 260 (ε/dm^3 mol^{-1} cm^{-1} 25 500), 300 (22 000); δ_H(250 MHz; [d_6]DMSO; Me_4Si) 1.62 (4 H, m, 2 × CH_2), 2.20 (1 H, m, 2′-H_α), 2.50 (4 H, m, 2 × C≡CH_2), 2.68 (1 H, m, 2′-H_β), 2.78 (1 H, m, C≡CH), 3.06 (5 H, m, 5′-H, NCH_3), 3.19 (3 H, s, NCH_3), 3.71 (3 H, s, OCH_3), 3.72 (3 H, s, OCH_3), 3.87 (1 H, m, 4′-H), 4.46 (1 H, m, 3′-H), 5.25 (1 H, d, *J* 4.5, 3′-OH), 6.47 (1 H, m, 1′-H), 6.80–7.35 (13 H, m, arom.H), 8.71 (1 H, s, N=CH) and 11.36 (1 H, s, NH).

1-{[2-Deoxy-5-*O*-(4,4′-dimethoxytriphenylmethyl)-3-*O*-[(2-cyanoethoxy)(*N*,*N*-diisopropylamino)phosphine)]-β-D-*erythro*-pentofuranosyl]}-6-[(dimethylamino)methylidene]amino-1,5-dihydro-3-(octa-1,7-diynyl)-4*H*-pyrazolo[3,4-*d*]pyrimidin-4-one (3a)

A soln. of **5a** (156 mg, 0.21 mmol) in dry CH_2Cl_2 (10 cm^3) was stirred with $(i\text{-Pr})_2NEt$ (0.07 cm^3, 0.42 mmol) at rt. Then, 2-cyanoethyl diisopropylphosphoramidochloridite (0.07 cm^3, 0.31 mmol) was added and the reaction mixture was stirred for 30 min. The solution was poured into 5% $NaHCO_3$ soln. (30 cm^3) and extracted with CH_2Cl_2 (3 × 30 cm^3). The combined organic phases were dried (Na_2SO_4) and the solvent was evaporated. The residual foam was applied to FC (silica gel, column 8 × 3 cm, eluted with CH_2Cl_2–acetone 100 : 0 → 85 : 15). Evaporation of the main zone afforded **3a** as colourless foam (125 mg, 63%) (Found: C, 65.81; H, 6.49; N, 11.95%. $C_{51}H_{61}N_8O_7P$ requires C, 65.93; H, 6.62; N, 12.06%); TLC (silica gel, CH_2Cl_2–acetone 85 : 15): R_f 0.6; δ_H(250 MHz; $CDCl_3$; Me_4Si) 1.16 (12 H, m, 4 × CH_3), 1.64 (6 H, m, CH_2CN), 2.15 (1 H, m, 2′-H_α), 2.19 (2H, m, C≡C-CH_2), 2.50 (3 H, m, 2′-H_β, C≡C-CH_2), 2.63 (1 H, m, C≡CH), 3.09 (3 H, m, NCH_3), 3.19 (3 H, s, NCH_3), 3.25 (2 H, m, $CH(CH_3)_2$), 3.76–3.77 (10 H, m, 2 × CH_3, OCH_2, 5′-H), 4.20 (1H, m, 4′-H), 4.72 (1 H, s, 3′-H), 6.59 (1 H, t, *J* 6.3, 1′-H), 6.75–7.55 (13 H, 3 m, arom.H), 8.39 (1 H, s, N=CH) and 8.74 ppm (1H, s, NH); δ_P(101 MHz; $CDCl_3$; H_3PO_4) 149.4 and 149.6.

1-(2-Deoxy-β-D-*erythro*-pentofuranosyl)-6-[(2-methylpropanoyl)amino]-1,5-dihydro-3-(octa-1,7-diynyl)-4*H*-pyrazolo[3,4-*d*]pyrimidin-4-one (4b)

Compound **2d** (100 mg, 0.21 mmol) was dried by coevaporation with pyridine, dissolved in DMF (1 cm^3) and 1,1,1,3,3,3-hexamethyldisilazane (0.5 cm^3) was added to the solution. The reaction mixture was stirred for 3 h at rt, then pyridine (1 cm^3) and isobutyric anhydride (1 cm^3, 6.03 mmol) were added. The solution was stirred overnight at rt, methanol (2 cm^3) was added under cooling (ice-bath) and stirring was continued for 1 h at rt. The solvent was evaporated, and the remaining oily residue was applied to FC (silica gel, column 8 × 3 cm, eluted with CH_2Cl_2–MeOH 100 : 0 → 95 : 5). Evaporation of the main zone afforded **4b** as colorless foam (106 mg, 89%) (Found: C, 59.87; H, 6.27; N, 15.67%. $C_{22}H_{27}N_5O_5$ requires C, 59.85; H, 6.16; N, 15.86%); TLC (silica gel, CH_2Cl_2–MeOH 9 : 1): R_f 0.45; λ_{max} (MeOH)/nm 252 (ε/dm^3 mol^{-1} cm^{-1} 20 700); δ_H(250 MHz; [d_6]DMSO; Me_4Si) 1.10–1.12 (6 H, s, $(CH_3)_2CH$), 1.62 (4 H, m, 2 × CH_2), 2.21 (5 H, m, 2′-H_α, 2 × C≡C-CH_2), 2.70 (1 H, m, 2′-H_β), 2.77 (2 H, s, C≡C*H*, $CH(CH_3)_2$), 3.44 (2 H, m, 5′-H), 3.78 (1 H, m, 4′-H), 4.38 (1 H, m, 3′-H), 4.74 (1 H, m, 5′-OH), 5.29 (1 H, m, 3′-OH), 6.36 (1 H, t, *J* 6.0, 1′-H) and 11.85 (2 H, s, 2 × NH).

1-(2-Deoxy-5-*O*-(4,4′-dimethoxytriphenylmethyl)-β-D-*erythro*-pentofuranosyl)-6-[(2-methylpropanoyl)amino]-1,5-dihydro-3-(octa-1,7-diynyl)-4*H*-pyrazolo[3,4-*d*]pyrimidin-4-one (5b)

Compound **4b** (195 mg, 0.44 mmol) was dried by repeated co-evaporation with pyridine and then dissolved in dry pyridine (3 cm^3). 4,4′-dimethoxytrityl chloride (196 mg, 0.58 mmol) and *N*,*N*-diisopropylethylamine (0.12 cm^3, 0.65 mmol) were added and the reaction mixture was stirred for 2 h at room temperature. The solution was poured into 5% aqueous $NaHCO_3$ (30 cm^3) and extracted with CH_2Cl_2, dried (Na_2SO_4) and evaporated to dryness. Co-evaporation with toluene (3 × 10 cm^3) afforded a foamy residue which was applied to FC (silica gel, column 10 × 4 cm, eluted with CH_2Cl_2–acetone 90 : 10). From the main zone **5b** was obtained as colourless foam (180 mg, 55%) (Found: C, 69.53; H, 6.01; N, 9.33%. $C_{43}H_{45}N_5O_7$ requires C, 69.43; H, 6.10; N, 9.42%); TLC (silica gel, CH_2Cl_2–acetone 9 : 1): R_f 0.22; λ_{max} (MeOH)/nm 235 (ε/dm^3 mol^{-1} cm^{-1} 34 200); δ_H(250 MHz; [d_6]DMSO; Me_4Si) 1.10–1.14 (6 H, s, $(CH_3)_2CH$), 1.63 (4 H, m, 2 × CH_2), 2.20 (4 H, m, 2 × C≡C-CH_2), 2.29 (1 H, m, 2′-H_α), 2.76–2.81 (2 H, m, 2′-H_β, $CH(CH_3)_2$), 2.97 (1 H, m, C≡CH), 3.05 (2 H, m, 5′-H), 3.71 (6 H, s, 2 × OCH_3), 3.90 (1 H, m, 4′-H), 4.48 (1 H, m, 3′-H), 5.31–5.33 (1 H, d, *J* 4.5, 3′-OH), 6.36 (1 H, t, *J* 4.3, 1′-H), 6.79 (6 H, m, 2 × OCH_3), 6.80–7.32 (13 H, 3 m, arom.H) and 11.92 (2 H, s, 2 × NH).

1-{[2-Deoxy-5-*O*-(4,4′-dimethoxytriphenylmethyl)-3-*O*-[(2-cyanoethoxy)(*N*,*N*-diisopropylamino)phosphino]-β-D-*erythro*-pentofuranosyl]}-6-[(2-methylpropanoyl)amino]-1,5-dihydro-3-(octa-1,7-diynyl)-4*H*-pyrazolo[3,4-*d*]pyrimidin-4-one (3b)

To a solution of **5b** (120 mg, 0.14 mmol) in dry CH_2Cl_2 (6 cm^3), $(i\text{-Pr})_2NEt$ (0.06 cm^3, 0.36 mmol) and 2-cyanoethyl diisopropylphosphoramidochloridite (0.06 cm^3, 0.23 mmol) were added. After 3 h, the solution was washed with saturated $NaHCO_3$ (20 cm^3), and extracted with CH_2Cl_2 (2 × 20 cm^3), the combined org. layer was

dried over Na_2SO_4 and evaporated. FC (silica gel, column 8 × 3 cm, eluted with CH_2Cl_2–acetone 98 : 2) afforded a colorless foam of **3b** (110 mg, 72%) (Found: C, 66.99; H, 6.65; N, 10.64%. $C_{52}H_{62}N_7O_7P$ requires C, 67.30; H, 6.73; N, 10.56%); TLC (silica gel, CH_2Cl_2–acetone 9 : 1): R_f 0.87; δ_H(250 MHz; $CDCl_3$; Me_4Si) 1.10 (6 H, m, $(CH_3)_2CH$), 1.16 (12 H, m, 4 × CH_3), 1.74 (6 H, m, 2 × CH_2, CH_2CN), 2.18 (1 H, m, 2′-H_α), 2.20 (2 H, m, C≡C-CH_2), 2.52 (4 H, m, 2′-H_β, C≡CH_2, $CH(CH_3)_2$), 2.67 (1 H, m, C≡CH), 3.63 (2 H, m, 5′-H), 3.77–3.79 (8 H, m, 2 × CH_3, OCH_2), 4.23 (1 H, m, 4′-H), 4.75 (1 H, m, 3′-H), 6.41 (1 H, t, *J* 6.3, 1′-H), 6.74–7.45 (13 H, 3 m, arom. H), 8.39 (1 H, s, N=CH) and 11.70 (1 H, s, NH); δ_P(101 MHz; $CDCl_3$; H_3PO_4) 149.0.

6-Amino-1-(2-deoxy-β-D-*erythro*-pentofuranosyl)-1,5-dihydro-3-(7-hydroxycoumarin-1′,2′,3′-triazol-4′-yl)pentylidyne-4*H*-pyrrolo[2,3-*d*]pyrimidin-4-one (17)

To a solution of **1** (368 mg, 1 mmol) and **15** (291 mg, 1.43 mmol) in water and ethyl alcohol (v/v = 1 : 1, 30 cm^3), a freshly prepared 1 M solution of sodium ascorbate (0.2 cm^3, 0.20 mmol) in water and copper(II) sulfate pentahydrate 7.5% in water (0.17 cm^3, 0.05 mmol) were added. The mixture was stirred vigorously overnight in the dark at rt for 15 h. The solvent was evaporated, and the remaining residue was loaded on a silica gel column FC (silica gel, column 10 × 4 cm, eluted with CH_2Cl_2–MeOH 80 : 20). From the main zone **17** was obtained as a yellow powder (300 mg, 53%); TLC (silica gel, CH_2Cl_2–MeOH 9 : 1): R_f 0.30; λ_{max} (MeOH)/nm 243 (ε/dm^3 mol^{-1} cm^{-1} 17 200), 347 (13 300); δ_H(250 MHz; [d_6]DMSO; Me_4Si) 1.60 (2 H, t, *J* 7.2, CH_2), 1.81 (2 H, t, *J* 7.4, CH_2), 2.08 (1 H, m, 2′-H_α), 2.30 (1 H, m, 2′-H_β), 2.41 (2 H, m, CH_2), 2.76 (2 H, t, *J* 7.3 Hz, C≡C-CH_2), 3.48 (1 H, m, 5′-H), 3.74 (1 H, m, 4′-H), 4.27 (1 H, m, 3′-H), 4.89 (1 H, m, 5′-OH), 5.19 (1 H, m, 3′-OH), 6.23 (1 H, t, *J* 6.0, 1′-H), 6.30 (2 H, s, NH_2), 6.85 (1 H, s, H-5-coumarin), 6.91 (1 H, m, H-6-coumarin), 7.70–7.74 (1 H, d, *J* 8.6, H-8-coumarin), 8.33 (1 H, s, H-5-triazole), 8.55 (1 H, s, H-4-coumarin) and 10.39 (1 H, s, HN); *m*/*z* (ESI-TOF) 596.18 (M + Na^+. $C_{28}H_{27}N_7O_7Na$ requires 596.20).

6-Amino-1-(2-deoxy-β-D-*erythro*-pentofuranosyl)-1,5-dihydro-3-(7-hydroxycoumarin-1′,2′,3′-triazol-4′-yl)pentylidyne-4*H*-pyrazolo[3,4-*d*]pyrimidin-4-one (16)

To a solution of **2d** (100 mg, 0.27 mmol) and **15** (55 mg, 0.27 mmol) in water and ethyl alcohol (v/v = 1 : 1, 8 cm^3), a freshly prepared 1 M solution of sodium ascorbate (0.054 cm^3, 0.054 mmol) in water and copper(II) sulfate pentahydrate 7.5% in water (0.045 cm^3, 0.0135 mmol) were added. The mixture was stirred vigorously in the dark at rt for 15 h. The solvent was evaporated, and the residue was applied to FC (silica gel, column 10 × 4 cm, eluted with CH_2Cl_2–MeOH 80 : 20). Evaporation of the main zone gave a yellow powder of **16** (140 mg, 90%). TLC (silica gel, CH_2Cl_2–MeOH 8 : 2): R_f 0.53; λ_{max} (MeOH)/nm 243 (ε/dm^3 mol^{-1} cm^{-1} 46 900), 347 (25 500); δ_H(250 MHz; [d_6]DMSO; Me_4Si) 1.62 (2 H, t, *J* 8.4, CH_2), 1.82 (2 H, t, *J* 8.9, CH_2), 2.14 (1 H, m, 2′-H_α), 2.50 (2 H, s, CH_2), 2.64 (1 H, m, 2′-H_β), 2.77 (2 H, t, *J* 8.4, C≡C-CH_2), 3.35 (2 H, m, 5′-H), 3.75 (1 H, m, 4′-H), 4.26 (1 H, m, 3′-H), 4.72 (1 H, m, 5′-OH), 5.22 (1 H, m, 3′-OH), 6.26 (1 H, t, *J* 7.9, 1′-H), 6.74 (2 H, s, NH_2), 6.84 (1 H, s, H-5-coumarin), 6.91 (1 H, m, H-6-coumarin), 7.71 (1 H, d, *J* 10.2, H-8-coumarin), 8.34 (1 H, s, H-5-triazole), 8.56 (1 H, s, H-4-coumarin), 10.68 (1 H, s, NH); *m*/*z* (ESI-TOF) 597.18 (M + Na^+. $C_{27}H_{26}N_8O_7Na$ requires 597.19).

Copper(I)-catalyzed [3 + 2] cycloaddition of oligonucleotides 12 or 13 with 3-azido-7-hydroxycoumarin 15

To the single-stranded oligonucleotide (5 A_{260} units), a 1 : 1 $CuSO_4$–TBTA ligand complex (0.05 cm^3 of a 20 mM stock solution in *t*-BuOH–H_2O 1 : 9), tris(carboxyethyl)phosphine (TCEP; 0.05 cm^3 of a 20 mM stock solution in water), 3-azido-7-hydroxycoumarin (**15**; 0.05 cm^3 of a 20 mM stock solution in dioxane–H_2O 1 : 1), sodium bicarbonate (0.05 cm^3 of a 20 mM aq. solution) and 0.035 cm^3 DMSO were added, and the reaction proceeded at room temperature for 12 h. The reaction mixture was concentrated in a speed vac and dissolved in 1 cm^3 bidistilled water and centrifuged for 20 min at 12 000 rpm. The supernatant solution was collected and further purified by reversed-phase HPLC in the trityl-off modus to give the 'click' product (oligonucleotide **18** or **19**). The molecular masses of **18** and **19** were determined by MALDI-TOF mass spectrometry (Table 7).

Acknowledgements

We thank Dr. V. R. Sirivolu for supplying us with compound **17** and Mr. P. Ding for Fig. 4d. We also thank Mr. D. Jiang for measuring the NMR spectra, Dr. T. Koch from Roche Diagnostics GmbH, Penzberg, Germany, for the measurement of the MALDI spectra and Mr. N. Q. Tran for the oligonucleotide syntheses. We appreciate critical reading by Mr. S. Pujari. Financial support by the Roche Diagnostics GmbH and ChemBiotech, Muenster, Germany, is gratefully acknowledged.

References

1 H. C. Kolb, M. G. Finn and K. B. Sharpless, *Angew. Chem., Int. Ed.*, 2001, **40**, 2004–2021.
2 H. C. Kolb and K. B. Sharpless, *Drug Discovery Today*, 2003, **8**, 1128–1137.
3 N. J. Agard, J. A. Prescher and C. R. Bertozzi, *J. Am. Chem. Soc.*, 2004, **126**, 15046–15047.
4 J. M. Langenhan and J. S. Thorson, *Curr. Org. Synth*, 2005, **2**, 59–81.
5 E. Delamarche, B. Michel, C. Gerber, D. Anselmetti, H.-J. Güntherodt, H. Wolf and H. Ringsdorf, *Langmuir*, 1994, **10**, 2869–2871.
6 M. J. Joralemon, R. K. O'Reilly, C. J. Hawker and K. L. Wooley, *J. Am. Chem. Soc.*, 2005, **127**, 16892–16899.
7 M. R. Whittaker, C. N. Urbani and M. J. Monteiro, *J. Am. Chem. Soc.*, 2006, **128**, 11360–11361.
8 J. E. Moses and A. D. Moorhouse, *Chem. Soc. Rev.*, 2007, **36**, 1249–1262.
9 D. D. Díaz, S. Punna, P. Holzer, A. K. McPherson, K. B. Sharpless, V. V. Fokin and M. G. Finn, *J. Polym. Sci. Part A: Polym. Chem.*, 2004, **42**, 4392–4403.
10 M. Malkoch, K. Schleicher, E. Drockenmuller, C. J. Hawker, T. P. Russell, P. Wu and V. V. Fokin, *Macromolecules (Washington, DC, U. S.)*, 2005, **38**, 3663–3678.
11 (*a*) P. M. E. Gramlich, C. T. Wirges, A. Manetto and T. Carell, *Angew. Chem., Int. Ed.*, 2008, **47**, 8350–8358, and references therein; (*b*) P. M. E. Gramlich, S. Warncke, J. Gierlich and T. Carell, *Angew. Chem., Int. Ed.*, 2008, **47**, 3442–3444; (*c*) J. Gierlich, G. A. Burley, P. M. E. Gramlich, D. M. Hammond and T. Carell, *Org. Lett.*, 2006, **8**, 3639–3642.
12 (*a*) A. J. Dirks, S. S. van Berkel, N. S. Hatzakis, J. A. Opsteen, F. L. van Delft, J. J. L. M. Cornelissen, A. E. Rowan, J. C. M. van Hest, F. P. J. T. Rutjes and R. J. M. Nolte, *Chem. Commun.*, 2005, 4172–4174; (*b*) S. S. Gupta, J. Kuzelka, P. Singh, W. G. Lewis, M. Manchester and M. G. Finn, *Bioconjugate Chem.*, 2005, **16**, 1572–1579; (*c*) A. Moulin, L. Demange, J. Ryan, D. Mousseaux, P. Sanchez, G. Bergé, D. Gagne,

D. Perrissoud, V. Locatelli, A. Torsello, J.-C. Galleyrand, J.-A. Fehrentz and J. Martinez, *J. Med. Chem.*, 2008, **51**, 689–693.
13 (*a*) P. Kočalka, A. H. El-Sagheer and T. Brown, *ChemBioChem*, 2008, **9**, 1280–1285; (*b*) R. Kumar, A. El-Sagheer, J. Tumpane, P. Lincoln, L. M. Wilhelmsson and T. Brown, *J. Am. Chem. Soc.*, 2007, **129**, 6859–6864; (*c*) A. El-Sagheer, R. Kumar, S. Findlow, J. M. Werner, A. N. Lane and T. Brown, *ChemBioChem*, 2008, **9**, 50–52.
14 F. Seela, V. R. Sirivolu and P. Chittepu, *Bioconjugate Chem.*, 2008, **19**, 211–224.
15 F. Seela, Y. He, J. He, G. Becher, R. Kröschel, M. Zulauf and P. Leonard, in *Methods in Molecular Biology*, ed. P. Herdewijn, Humana Press, Totowa, NJ, 2004, vol. 288, pp. 165–86.
16 F. Seela and G. Becher, *Synthesis*, 1998, 207–214.
17 F. Seela and G. Becher, *Chem. Commun.*, 1998, 2017–2018.
18 J. He and F. Seela, *Nucleic Acids Res.*, 2002, **30**, 5485–5496.
19 G. Becher, J. He and F. Seela, *Helv. Chim. Acta*, 2001, **84**, 1048–1065.
20 J. He and F. Seela, *Tetrahedron*, 2002, **58**, 4535–4542.
21 F. Seela and G. Becher, *Helv. Chim. Acta*, 1999, **82**, 1640–1655.
22 F. Seela and G. Becher, *Nucleic Acids Res.*, 2001, **29**, 2069–2078.
23 F. Seela and M. Zulauf, *Synthesis*, 1996, 726–730.
24 F. Seela and V. R. Sirivolu, *Helv. Chim. Acta*, 2007, **90**, 535–552.
25 F. Seela and K. I. Shaikh, *Tetrahedron*, 2005, **61**, 2675–2681.
26 F. Seela and H. Steker, *Helv. Chim. Acta*, 1986, **69**, 1602–1613.
27 F. Seela and M. Zulauf, *Helv. Chim. Acta*, 1999, **82**, 1878–1898.
28 F. Seela and V. R. Sirivolu, *Chem. Biodiversity*, 2006, **3**, 509–514.
29 K. Sivakumar, F. Xie, B. M. Cash, S. Long, H. N. Barnhill and Q. Wang, *Org. Lett.*, 2004, **6**, 4603–4606.
30 F. Seela and V. R. Sirivolu, *Org. Biomol. Chem*, 2008, **6**, 1674–1687.
31 C. A. M. Seidel, A. Schulz and M. H. M. Sauer, *J. Phys. Chem.*, 1996, **100**, 5541–5553.
32 G. Wenska and S. Paszyc, *Can. J. Chem.*, 1988, **66**, 513–516.
33 S. A. E. Marras, F. R. Kramer and S. Tyagi, *Nucleic Acids Res.*, 2002, **30**, e122.
34 N. Ramzaeva, H. Rosemeyer, P. Leonard, K. Mühlegger, F. Bergmann, H. von der Eltz and F. Seela, *Helv. Chim. Acta*, 2000, **83**, 1108–1126.
35 F. Seela, K. Shaikh and H. Eickmeier, *Acta Crystallogr. Sect. C: Cryst. Struct. Commun.*, 2004, **60**, o489–o491.
36 M. Torimura, S. Kurata, K. Yamada, T. Yokomaku, Y. Kamagata, T. Kanagawa and R. Kurane, *Anal. Sci.*, 2001, **17**, 155–160.
37 A. P. de Silva, H. Q. N. Gunaratne, T. Gunnlaugsson, A. J. M. Huxley, C. P. McCoy, J. T. Rademacher and T. E. Rice, *Chem. Rev. (Washington, DC, U. S.)*, 1997, **97**, 1515–1566.
38 J. M. Prober, G. L. Trainor, R. J. Dam, F. W. Hobbs, C. W. Robertson, R. J. Zagursky, A. J. Cocuzza, M. A. Jensen and K. Baumeister, *Science (Washington, DC, U. S.)*, 1987, **238**, 336–341.
39 C. Seidel, K. Rittinger, J. Cotés, R. S. Goody, M. Köllner, J. Wolfrum and K. O. Greulich, in *Biomolecular Spectroscopy II*, ed. R. R. Birge and L. A. Nafie, Proc. SPIE, 1991, vol. 1432, pp. 105–116.
40 M. Petersheim and D. H. Turner, *Biochemistry*, 1983, **22**, 256–263.